

# Ghrelin-Induced Sodium Reabsorption Is Mediated by PKA and Microtubule-Dependent $\alpha\text{E}_{\text{Na}}\text{C}$ Translocation in Female Rats

Brandon A. Kemp,<sup>1</sup> Nancy L. Howell,<sup>1</sup> John J. Gildea,<sup>2</sup> and Shetal H. Padia<sup>1</sup>

<sup>1</sup>Department of Medicine, Division of Endocrinology and Metabolism, University of Virginia Health System, Charlottesville, Virginia 22908; and <sup>2</sup>Department of Pathology, University of Virginia Health System, Charlottesville, Virginia 22908

ORCID numbers: 0000-0002-0609-3557 (B. A. Kemp); 0000-0001-8326-3129 (S. H. Padia).

Intrarenal ghrelin infusion activates ghrelin receptors in the kidney collecting duct (CD) to increase  $\alpha$  epithelial sodium ( $\text{Na}^+$ ) channel ( $\alpha\text{E}_{\text{Na}}\text{C}$ )-dependent  $\text{Na}^+$  reabsorption *in vivo*, but the underlying mechanisms are unknown. Seventy-two hours following uninephrectomy, 12-week-old female Sprague-Dawley rats received the following renal interstitial (RI) infusions for 1 hour after a 1-hour control: vehicle (n = 10), ghrelin (3  $\mu\text{g}/\text{minute}$ ; n = 8), ghrelin + phosphatidylinositol 3-kinase (PI3K) inhibitor LY-294002 (0.1  $\mu\text{g}/\text{kg}/\text{minute}$ ; n = 7), ghrelin + protein kinase A (PKA) inhibitor adenosine 3'/5'-cyclic monophosphorothioate, Rp-isomer (10  $\mu\text{g}/\text{kg}/\text{minute}$ ; n = 8), ghrelin + microtubule polymerization inhibitor nocodazole (0.3  $\mu\text{g}/\text{kg}/\text{minute}$ ; n = 7), or ghrelin + actin polymerization inhibitor cytochalasin D (0.3  $\mu\text{g}/\text{kg}/\text{minute}$ ; n = 6). Compared with vehicle infusion, RI ghrelin induced a significant anti-natriuresis (urine  $\text{Na}^+$  excretion was reduced by  $53.7\% \pm 6.8\%$ ;  $P < 0.001$ ). This effect was abolished during concomitant PKA or microtubule inhibition ( $106.4\% \pm 9.4\%$  and  $109.7\% \pm 10.6\%$  of vehicle infusion, respectively;  $P < 0.01$  from ghrelin) but not during concomitant PI3K or actin inhibition (reduced by  $48.6\% \pm 3.9\%$  and  $52.8\% \pm 12.7\%$ , respectively;  $P < 0.001$  and  $P < 0.01$  from vehicle, respectively;  $P =$  not significant from ghrelin). Infusions had no effect on mean arterial pressure. Western blot analysis demonstrated that CD membrane but not total  $\alpha\text{E}_{\text{Na}}\text{C}$  expression increased in response to ghrelin infusion compared with vehicle, ( $0.39 \pm 0.05$  vs  $0.12 \pm 0.02$  arbitrary units;  $P < 0.01$ ). This effect was abolished during PKA or microtubule inhibition but persisted during PI3K or actin inhibition. Neural precursor cell expressed, developmentally down-regulated 4 isoform 2 (Nedd4-2) dependent internalization of  $\alpha\text{E}_{\text{Na}}\text{C}$  was not affected by ghrelin, indicating that microtubule-dependent forward trafficking of  $\alpha\text{E}_{\text{Na}}\text{C}$  is necessary for anti-natriuretic responses to ghrelin. Taken together, these studies highlight the importance of PKA and microtubule polymerization in ghrelin-induced  $\alpha\text{E}_{\text{Na}}\text{C}$ -mediated  $\text{Na}^+$  reabsorption.

Copyright © 2019 Endocrine Society

This article has been published under the terms of the Creative Commons Attribution Non-Commercial, No-Derivatives License (CC BY-NC-ND; <https://creativecommons.org/licenses/by-nc-nd/4.0/>).

**Freeform/Key Words:** ghrelin, sodium,  $\text{E}_{\text{Na}}\text{C}$ , trafficking, kidney, hypertension

Reductions in renal sodium ( $\text{Na}^+$ ) excretory capacity and marked increases in cumulative  $\text{Na}^+$  balance often contribute to the development of primary hypertension. Ghrelin is a 28-

Abbreviations: AKT, protein kinase B; Ang II, angiotensin II; AQP-2, aquaporin-2; AU, arbitrary unit; BCA, bicinchoninic acid; CD, collecting duct; CTD, cytochalasin D; D<sub>5</sub>W, 5% dextrose in water;  $\text{E}_{\text{Na}}\text{C}$ , epithelial sodium channel; GR, glucocorticoid receptor; IMCD, inner-medullary collecting duct; L<sub>1</sub>CAM, L<sub>1</sub> cell-adhesion molecule; LY, LY-294002; MAP, mean arterial pressure;  $\text{Na}^+$ , sodium; Nedd4-2, neural precursor cell expressed, developmentally down-regulated 4 isoform 2; NOC, nocodazole; pAKT, phosphorylation of protein kinase B; PI3K, phosphatidylinositol 3-kinase; PKA, protein kinase A; pNedd4-2, phosphorylation of Nedd4-2; pSGK<sub>1</sub>, phosphorylation of serum and glucocorticoid-regulated kinase 1; RI, renal interstitial; Rp-cAMPS, adenosine 3'/5'-cyclic monophosphorothioate, Rp-isomer; RT, room temperature; SGK<sub>1</sub>, serum and glucocorticoid-regulated kinase 1; TBS, Tris-buffered saline; TBS<sup>1</sup>, Tris-buffered saline with 0.1% Tween-20; TBS<sup>2</sup>, Tris-buffered saline with 0.02% Tween-20;  $\text{U}_{\text{Na}}\text{V}$ , urine sodium excretion.

amino acid peptide hormone, originally discovered as an appetite-stimulating hormone secreted by the stomach and small intestine. Circulating ghrelin levels increase before meals and decrease following food ingestion. Hypothalamic ghrelin receptors mediate these orexigenic effects, but recent studies have also confirmed widespread distribution of ghrelin receptors in tissues relevant to cardiovascular control, including the kidney. Furthermore, ghrelin itself is also produced by the kidney and functions to increase  $\text{Na}^+$  reabsorption [1–4]. Chronic genetic inhibition of intrarenal but not systemic glucocorticoid receptor (GR) activity has been shown to ameliorate both high-fat diet [2]- and angiotensin II (Ang II) [4]-induced hypertension in rodents. These effects are mediated, in part, by reductions in epithelial  $\text{Na}^+$  channel ( $\text{E}_{\text{NaC}}$ )-dependent  $\text{Na}^+$  reabsorption in response to GR inhibition [2, 4]. However, little is known about the underlying signaling pathways that link renal GRs to  $\text{E}_{\text{NaC}}$  in the kidney and serve as the central purpose of the current investigation.

Previous studies have shown that intrarenal GRs localize to the collecting duct (CD), where they couple to an adenylyl cyclase second messenger system to increase renal interstitial (RI) cAMP levels and induce  $\text{E}_{\text{NaC}}$ -dependent  $\text{Na}^+$  reabsorption *in vivo* [1, 3]. Serum and glucocorticoid-regulated kinase 1 (SGK<sub>1</sub>) is a common upstream signaling intermediate regulating  $\text{E}_{\text{NaC}}$  [5, 6], and phosphorylation leads to SGK<sub>1</sub> activation (pSGK<sub>1</sub>) [7, 8]. cAMP is known to induce pSGK<sub>1</sub> via two different pathways: (i) protein kinase A (PKA) [9, 10] and (ii) phosphatidylinositol 3-kinase (PI3K) [11]. Renal GR-mediated  $\text{Na}^+$  reabsorption is accompanied by increased pSGK<sub>1</sub>, but whether this effect is dependent on PKA or PI3K in the CD is unknown.

The amiloride-sensitive  $\text{E}_{\text{NaC}}$  channel is the main  $\text{Na}^+$  transporter of the CD.  $\text{E}_{\text{NaC}}$  is composed of three subunits,  $\alpha$ ,  $\beta$ , and  $\gamma$ , which intercalate to form the channel pore. Of the three subunits, the  $\alpha\text{E}_{\text{NaC}}$  subunit alone is critical to the formation of a functional channel. This is because the expression of  $\alpha\text{E}_{\text{NaC}}$  alone in *Xenopus* oocytes confers a low amiloride-sensitive  $\text{Na}^+$  current, whereas neither the  $\beta$  nor the  $\gamma$  subunits can form functional conducting channels when expressed alone.  $\beta$ - and  $\gamma\text{E}_{\text{NaC}}$ , however, do help maximize channel activity [12, 13]. We recently reported that acute RI ghrelin infusion increased CD outer membrane targeting of  $\alpha\text{E}_{\text{NaC}}$  without changing total  $\alpha\text{E}_{\text{NaC}}$  protein expression [1]. Renal blockade of  $\text{E}_{\text{NaC}}$  with amiloride abolished the ability of ghrelin to increase  $\text{Na}^+$  reabsorption, indicating that GRs stimulate  $\text{Na}^+$  reabsorption via  $\text{E}_{\text{NaC}}$ .

One way of regulating  $\text{E}_{\text{NaC}}$  activity is by affecting the abundance of protein in the membrane of CD cells via factors that induce trafficking to, or promote stability at, the cell surface [14]. The stimulatory effect of pSGK<sub>1</sub> on  $\alpha\text{E}_{\text{NaC}}$  surface abundance is conventionally attributed to a decrease in  $\text{E}_{\text{NaC}}$  channel removal from the plasma membranes of CD cells via interference with the  $\text{E}_{\text{NaC}}$ -neural precursor cell expressed, developmentally down-regulated 4 isoform 2 (Nedd4-2) interaction [15]. This ultimately leads to an accumulation of  $\text{E}_{\text{NaC}}$  channels at the plasma membrane and resultant  $\text{Na}^+$  reabsorption. However, pSGK<sub>1</sub> can directly induce the insertion of  $\alpha\text{E}_{\text{NaC}}$  into the plasma membrane via specific components of the cytoskeleton, such as microtubules [16] or actin [17]. This functional work has established the central role of recycling in the regulation of  $\text{E}_{\text{NaC}}$ , not only in promoting channel surface stability but also in maintaining the intracellular channel pool(s) that permit a redistribution of  $\text{E}_{\text{NaC}}$  to the plasma membrane in response to hormonal regulators. Despite these advances, we know much more about the regulation of apical channel density by inhibition of endocytic processes than we do about the factors that promote  $\text{E}_{\text{NaC}}$  forward trafficking. The present investigations indicate that ghrelin-induced  $\text{Na}^+$  reabsorption is mediated by PKA, resulting in increased pSGK<sub>1</sub> and microtubule-dependent forward trafficking of  $\alpha\text{E}_{\text{NaC}}$  to the outer membranes of CD cells in normal rats.

## 1. Materials and Methods

All experimental protocols were approved by the Animal Care and Use Committee at the University of Virginia and performed in accordance with the National Institutes of Health Guide for the Care and Use of Laboratory Animals.

## A. General Protocols

### A-1. Animal preparation

The experiments were conducted on 12-week-old female Sprague-Dawley rats (Envigo; n = 77), housed in a vivarium under controlled conditions (temperature  $21 \pm 1^\circ\text{C}$ ; humidity  $60\% \pm 10\%$ ; light 8:00 to 20:00) and fed a normal  $\text{Na}^+$  diet (0.30%  $\text{Na}^+$ ).

Rats were placed under short-term anesthesia with isoflurane, and a retroperitoneal flank incision was made to remove the right kidney using a sterile technique. After a 72-hour recovery, the rats were anesthetized with Inactin (100 mg/kg body weight) via an IP injection, and a tracheostomy was performed to assist respiration. Direct cannulation of the right internal jugular vein with PE-10 tubing provided IV access through which vehicle 5% dextrose in water ( $\text{D}_5\text{W}$ ) was infused at  $20 \mu\text{L}/\text{minute}$ . Direct cannulation of the right carotid artery with PE-50 tubing provided arterial access for monitoring mean arterial pressure (MAP). Following a midline laparotomy, a microcatheter (PE-10) was inserted into the ureter of the remaining kidney (left) to collect urine for the quantification of urine  $\text{Na}^+$  excretion ( $\text{U}_{\text{NaV}}$ ).

### A-2. Renal cortical interstitial infusion

An open bore microinfusion catheter (PE-10) was inserted under the renal capsule into the cortex of the remaining kidney (left) to ensure the RI infusion of vehicle  $\text{D}_5\text{W}$  or pharmacological agent(s) at  $2.5 \mu\text{L}/\text{minute}$  with a syringe pump (model 55-222; Harvard). When more than one agent was simultaneously infused, separate interstitial catheters were used. Vetbond tissue adhesive (3M Animal Care Products) was added to secure the catheter(s) and prevent interstitial pressure loss in the kidney.

### A-3. Blood pressure measurements

MAP was measured by the direct intracarotid method (see above) with the use of a digital blood pressure analyzer (Micromed, Inc.). MAPs were recorded every 5 minutes and averaged for all periods. Experiments were initiated at the same time each day to prevent any diurnal variation in blood pressure.

## B. Pharmacological Agents

### B-1. Rat acyl ghrelin (3 $\mu\text{g}/\text{minute}$ ; Tocris)

The dose of acyl ghrelin was based on the tenets that the normal rat kidney receives  $\approx 20\%$  to  $25\%$  of the cardiac output and that the volume of RI fluid in a normal rat kidney is  $\approx 350 \mu\text{L}$ . Thus, acyl ghrelin was calculated at one-fourth of the dose given systemically to decrease MAP in normal subjects, corrected for the volume of distribution in the rat cortical interstitium. Adenosine 3'5'-cyclic monophosphorothioate, Rp-isomer (Rp-cAMPS;  $10 \mu\text{g}/\text{kg}/\text{minute}$ ; Calbiochem), was used to inhibit PKA. LY-294002 (LY;  $0.1 \mu\text{g}/\text{kg}/\text{minute}$  for *in vivo* studies and  $72 \mu\text{M}$  for *in vitro* cell culture experiments; Cell Signaling) was used to inhibit PI3K. The LY dose of  $72 \mu\text{M}$  was chosen for *in vitro* studies, as it reflects the total amount of LY that the rats received into the kidney during the *in vivo* experiments. Specifically, a total of  $1.5 \mu\text{g}$  was infused over a 1-hour experimental period into the kidney during the *in vivo* experiments ( $0.1 \mu\text{g} \times 0.250 \text{ kg} \times 60 \text{ minutes} = 1.5 \mu\text{g}$ ), which was distributed in roughly  $68 \mu\text{L}$  fluid (the volume of fluid in the kidney interstitium of a rat). This equates to  $\sim 22 \text{ mg}/\text{L}$  LY, which corresponds to a dose of  $\sim 72 \mu\text{M}$  for the cellular experiments. Nocodazole (NOC;  $3 \mu\text{g}/\text{kg}/\text{minute}$ ; Sigma) was used to inhibit microtubule polymerization. Cytochalasin D (CTD;  $0.3 \mu\text{g}/\text{kg}/\text{minute}$ ; Sigma) was used to inhibit actin polymerization. Insulin ( $100 \text{ nM}$ ; Humulin R  $100 \text{ U}/\text{mL}$ ; Eli Lilly) was used to stimulate insulin receptors in

mouse inner-medullary CD (IMCD) cells. Insulin is known to stimulate insulin receptors in IMCD cells through the PI3K signaling pathway via phosphorylation of protein kinase B (AKT) at Ser 473 (pAKT). IMCD cells were treated with insulin  $\pm$  LY to determine if the dose of LY used in the *in vivo* studies could successfully inhibit insulin-induced pAKT, thereby serving as a positive control.

### C. Kidney Homogenate and Western Blot Analysis

One-half of the kidney was homogenized (Polytron at setting 6, 3  $\times$  5-second pulses) in detergent-free buffer (10 mM Tris, 200 mM sucrose, 1 mM EDTA, pH 7.4) with Halt protease and phosphatase inhibitor cocktail (Thermo Scientific) and spun at 900 *g* for 10 minutes at 4°C to remove cellular debris. The supernatant was removed, and total protein was quantified using a bicinchoninic acid (BCA) assay (Pierce). SDS samples were prepared and separated by SDS-PAGE (10% TGX Stain-Free gels; 40  $\mu$ g protein loaded per lane) and underwent the UV crosslinking procedure for 45 seconds with the ChemiDoc MP Imaging System (BioRad), following BioRad's specific protocol. The samples were then transferred onto a nitrocellulose membrane, blocked in 5% milk in Tris-buffered saline (TBS) with 0.1% Tween-20 (TBST<sup>1</sup>) for 2 hours at 4°C, and then incubated overnight at 4°C with the following primary antibodies made in 5% milk TBST<sup>1</sup>:  $\alpha$ E<sub>Na</sub>C (1:500; Cat. #ASC-030; RRID: [AB\\_10917439](#); Alomone Labs) [18], SGK (1:3000; Cat. #S5188; RRID: [AB\\_477521](#); Sigma) [19], and total Nedd4-2 (1:1000; Cat. #ab46521; RRID: [AB\\_2149325](#); abcam) [20] or in 5% BSA in TBST: pSGK<sub>1</sub> ser 78 (1:1000; Cat. #5599; RRID: [AB\\_10698593](#); Cell Signaling Technology) [21] and phosphorylated Nedd4-2 ser 448 (pNedd4-2; 1:1000; Cat. #ab168349; RRID: [AB\\_2801582](#); abcam) [22]. Membranes were subsequently incubated with their respective horseradish peroxidase-conjugated secondary antibodies (1:2500; Cat. #NA934V; RRID: [AB\\_772210](#); GE Healthcare) [23] or NA931V (RRID: [AB\\_772206](#)) [24] for 2 hours at room temperature (RT). Signals were detected using chemiluminescence with the ChemiDoc MP Imaging System, and band intensities were measured with ImageJ software (National Institutes of Health). All blots were normalized to total protein.

### D. CD Isolation and Western Blot Analysis

After total protein was determined by the BCA assay from the kidney homogenate (obtained from one-half of a kidney, as stated above), 1 mg of kidney homogenate was resuspended in 1 mL of detergent-free buffer and incubated with the cell-adhesion CD-specific marker, L<sub>1</sub> cell-adhesion molecule (L<sub>1</sub>CAM; 4  $\mu$ L, 1 mg/mL final concentration; Cat. #ab24345; RRID: [AB\\_448025](#); abcam) [25] on a 360° rocker for 2 hours at RT. L<sub>1</sub>CAM is expressed only in membranes of CD cells, allowing for >95% purification of CD membranes [26]. A total of 10  $\mu$ L magnetic protein A/G beads (Pierce) was added and incubated on a 360° rocker for 30 minutes at RT, followed by three washes in PBS. The CD affinity-attached membranes were eluted by the incubation of the beads with 125  $\mu$ L of  $\times$ 2 sample buffer in a rocker for 10 minutes at RT. The samples were separated by SDS-PAGE (10% TGX Stain-Free gels; 20  $\mu$ L loaded per lane) and underwent the UV crosslinking procedure, as stated previously. The samples were then transferred onto a nitrocellulose membrane, incubated with  $\alpha$ E<sub>Na</sub>C (1:500) [18], and followed the remaining Western procedure described above.

### E. In Vivo Kidney Perfusion and Fixation Procedure

Following the RI infusion of vehicle or pharmacological agent, the rat heart left-ventricular cavity was cannulated, and the rat was perfused with 40 mL cold 4% sucrose in PBS followed by 40 mL cold 4% paraformaldehyde in PBS. The kidneys were sliced in half and placed in 4% paraformaldehyde for 2 hours at RT. The slices were rinsed three times in PBS, immersed in 100 mM Tris-HCl for 30 minutes, and then rinsed three times in PBS before being stored in 30% sucrose in PBS overnight at 4°C. The next day, the kidney slices were embedded in Tissue Tek OCT Compound in Cryomold vinyl specimen molds, placed at  $-20^{\circ}\text{C}$  until frozen,

and then stored at  $-80^{\circ}\text{C}$  until processing. Cryostat thin sections (5 to 8  $\mu\text{m}$ ) were placed on Probe On Plus positively charged microscope slides through the University of Virginia Research Histology Core and immediately stained.

#### *F. Confocal Immunofluorescence Microscopy*

After the kidney sections had been spotted onto slides and washed three times with TBS, they followed one of two protocols for permeabilization. For protocol 1, the sections were permeabilized with either 0.2% or 0.5% Triton-X in TBS for 10 minutes, and for protocol 2, the sections were permeabilized with 100% cold methanol at  $-20^{\circ}\text{C}$  for 10 minutes. The sections were then washed three times in TBST<sup>2</sup> (0.02% Tween-20) and then blocked in 1% milk TBST<sup>2</sup> for 1 hour at RT. The kidney sections were incubated with primary antibodies in 1% milk TBST overnight at  $4^{\circ}\text{C}$ . After washing three times in TBST<sup>2</sup>, Alexa 647-conjugated donkey anti-rabbit and Alexa 488-conjugated donkey anti-mouse secondary antibodies (1:500; Cat. #A31573; RRID:AB\_2536183 [27] and Cat. #A21202; RRID:AB\_141607 [28]; Invitrogen) and/or Hoechst 33342 (1:2000; Cat. #H3570; Molecular Probes) were added in 1% milk TBST<sup>2</sup> for 1 hour at RT. The following antibody pair was permeabilized with 0.5% Triton-X: aquaporin-2 (AQP-2; 1:2000; Cat. #ab15116; RRID:AB\_301662); abcam) [29] and  $\alpha$ -tubulin (1:1000; Cat. #T6199; RRID:AB\_477583; Sigma) [30]. The following antibody pair was permeabilized with 0.2% Triton-X:  $\alpha\text{E}_{\text{NaC}}$  (1:100; Cat. #sc-21012; RRID:AB\_2285600; Santa Cruz Biotechnology) [31], AQP-2 (1:100; Cat. #sc-515770; RRID:AB\_2810957; Santa Cruz Biotechnology) [32], and Hoechst (1:2000). The following antibodies were permeabilized with 100% cold methanol: AQP-2 (1:100; Santa Cruz Biotechnology) [32] and  $\beta$ -actin (1:500; Cat. #4970; RRID:AB\_2223172; Cell Signaling Technology) [33]. Following secondary antibody incubation, the slices were washed three times in TBST, Fluoromount G (SouthernBiotech) was applied, and the specimens were covered with a glass coverslip. Stained CDs were photographed under epifluorescence illumination using an automated Olympus IX81 spinning disk confocal microscope using a 60 $\times$  Plan Apo 5 water immersion objective with a numeric aperture of 1.2. The microscope was controlled using Slidebook 5.5 software (3i), and 5  $\mu$ -thick z-stack images were captured using a Hamamatsu electron-multiplying charge-coupled device camera at 0.25  $\mu$  intervals and deconvolved using the autoquant spinning-disk deconvolution module.  $\alpha\text{E}_{\text{NaC}}$  cortical CD apical membrane expression was quantitated in ImageJ by opening two mid z-stack images—one autofluorescence and the other  $\alpha\text{E}_{\text{NaC}}$  expression—and used the Sync Windows feature of ImageJ. A 4  $\mu^2$  measuring window was aligned directly adjacent to the most apical border of the cell using the autofluorescence channel, and the  $\alpha\text{E}_{\text{NaC}}$  fluorescence was measured within this same synchronized window. The immunoreactive  $\alpha$ -tubulin and  $\beta$ -actin fluorescence intensity was calculated as total intracellular fluorescence intensity within the CD. For all confocal analysis, quantifications were performed on eight CD cells with four measurements taken per tubule from a rat and averaged.

#### *G. Cell Culture*

IMCD cells were purchased from American Type Culture Collection and cultured in DMEM F-12 media (Gibco), supplemented with 5% fetal bovine serum (Genesee Scientific) and 1% penicillin/streptomycin (Genesee Scientific) at  $37^{\circ}\text{C}$  and 5%  $\text{CO}_2$ . Experiments were conducted in six-well cell culture-treated plates (Falcon) and performed in triplicates. Once the cells reached 70% to 75% confluence, they were serum starved overnight (18 hours) and then studied with all drug treatments performed in serum-free media. After drug treatment, the cells were rinsed two times in PBS, and then 125  $\mu\text{L}$  mammalian protein extraction reagent (Thermo Scientific) with phosphatase and protease inhibitors was added to each well of the six-well plate. The cells were scraped and then sonicated 3  $\times$  5 pulses on the lowest setting. A BCA assay was performed to measure total protein, and 10  $\mu\text{g}$  protein was loaded per lane. The remaining Western blot procedure was followed, as mentioned previously. The blots were probed with pAKT (1:10,000; Cat. #4060S; RRID:AB\_2315049; Cell Signaling Technology)

[34] made up in 5% BSA in TBST or total AKT (1:1000; Cat. #9272S; RRID:AB\_329827; Cell Signaling Technology) [35] made up in 5% milk TBST and then normalized to total protein transferred.

### H. Statistical Analyses

Data are presented as means  $\pm$  1 SE. Statistical significance was determined by using one-way ANOVA, followed by Tukey multiple comparisons with 95% confidence using Prism GraphPad software. Significance level was set at  $P < 0.05$ .

### I. Specific Protocols

#### I-1. Effects of acute intrarenal PKA or PI3K inhibition combined with RI ghrelin infusion on $U_{Na}V$ and MAP and on CD $\alpha E_{Na}C$ and kidney homogenate $\alpha E_{Na}C$ , pSGK<sub>1</sub>, and SGK protein expression

Following a 1-hour equilibration and 1-hour control period, the following groups of rats were studied: (i) Control (n = 10). Kidney received RI infusion of D<sub>5</sub>W for 1 hour. (ii) Ghrelin (n = 8). Kidney received RI infusion of ghrelin (3  $\mu$ g/minute) for 1 hour. (iii) Ghrelin + Rp-cAMPS (n = 10). Kidney received RI coinfusion of ghrelin + Rp-cAMPS (10  $\mu$ g/kg/minute) for 1 hour. (iv) Rp-cAMPS (n = 8). Kidney received RI infusion of Rp-cAMPS for 1 h. (v) Ghrelin + LY (n = 7). Kidney received RI infusion of ghrelin + LY (0.1  $\mu$ g/kg/minute) for 1 hour. (vi) LY (n = 5). Kidney received RI infusion of LY for 1 hour.  $U_{Na}V$  and MAP were measured for each period. Kidneys from control, ghrelin, ghrelin + Rp-cAMPS, and ghrelin + LY (n = 6 for each condition) were harvested at the end of the study and processed for Western blot analysis. In a separate set of animals, a representative rat for each of the four previously listed conditions was perfused separately and processed for confocal microscopy measuring  $\alpha E_{Na}C$  expression.

#### I-2. Effects of insulin in the presence and absence of LY on pAKT and total AKT protein expression in IMCD cells

IMCD cells were treated as follows in triplicates performed in two separate experiments: (i) Control. Serum-free media containing 0.7% dimethyl sulfoxide. (ii) Insulin. Insulin (100 nM) in serum-free medium containing 0.7% dimethyl sulfoxide for 5 minutes. (iii) Insulin + LY. Thirty minutes pretreatment with LY (72  $\mu$ M), followed by cotreatment with insulin + LY for 5 minutes. (iv) LY Alone. LY for 35 minutes.

#### I-3. Effects of acute intrarenal microtubule or actin polymerization inhibition combined with RI ghrelin infusion on $U_{Na}V$ and MAP and on CD $\alpha E_{Na}C$ and kidney homogenate $\alpha E_{Na}C$ , pSGK<sub>1</sub>, SGK, pNedd4-2, and Nedd4-2 protein expression

Following a 1-hour equilibration and 1-hour control period, the following groups of rats were studied: (i) Control (n = 10). Kidney received RI infusion of D<sub>5</sub>W for 1 hour. (ii) Ghrelin (n = 8). Kidney received RI infusion of ghrelin (3  $\mu$ g/minute) for 1 hour. (iii) Ghrelin + NOC (n = 7). Kidney received RI coinfusion of ghrelin + NOC (3  $\mu$ g/kg/minute) for 1 hour. (iv) NOC (n = 6). Kidney received RI infusion of NOC for 1 hour. (v) Ghrelin + CTD (n = 6). Kidney received RI infusion of ghrelin + CTD (0.3  $\mu$ g/kg/minute) for 1 hour. (vi) CTD (n = 6). Kidney received RI infusion of CTD for 1 hour.  $U_{Na}V$  and MAP were measured for each period. Kidneys from control, ghrelin, ghrelin + NOC, and ghrelin + CTD (n = 6 for each condition) were harvested at the end of the study and processed for Western blot analysis. In a separate set of animals, a representative rat for each of the four previously listed conditions was perfused separately and processed for confocal microscopy measuring  $\alpha E_{Na}C$  expression. Confocal microscopy was also used to verify microtubule and actin polymerization inhibition by measuring  $\alpha$ -tubulin and  $\beta$ -actin, respectively.

## 2. Results

### A. Ghrelin-Induced Anti-Natriuresis Is Abolished in the Presence of PKA Inhibition but Persists During PI3K Inhibition Without Affecting MAP

Figure 1 shows the  $U_{Na}V$  and MAP data in the following groups: vehicle control D<sub>5</sub>W (n = 10), ghrelin (3  $\mu$ g/minute; n = 8), ghrelin + PKA inhibitor Rp-cAMPS (10  $\mu$ g/kg/minute; n = 9), ghrelin + PI3K inhibitor LY (0.1  $\mu$ g/kg/minute; n = 7), Rp-cAMPS alone (n = 8), or LY alone (n = 5). In Fig. 1A RI ghrelin infusion induced a significant anti-natriuresis compared with the vehicle control experimental period ( $U_{Na}V$  was reduced by  $53.7\% \pm 6.8\%$ ;  $P < 0.001$ ). This effect was abolished during concomitant PKA inhibition with Rp-cAMPS. During ghrelin + PI3K inhibition, ghrelin-induced anti-natriuresis persisted ( $U_{Na}V$  was reduced by  $48.6\% \pm 3.9\%$  from the vehicle control experimental period;  $P < 0.01$ ). Neither Rp-cAMPS nor LY had

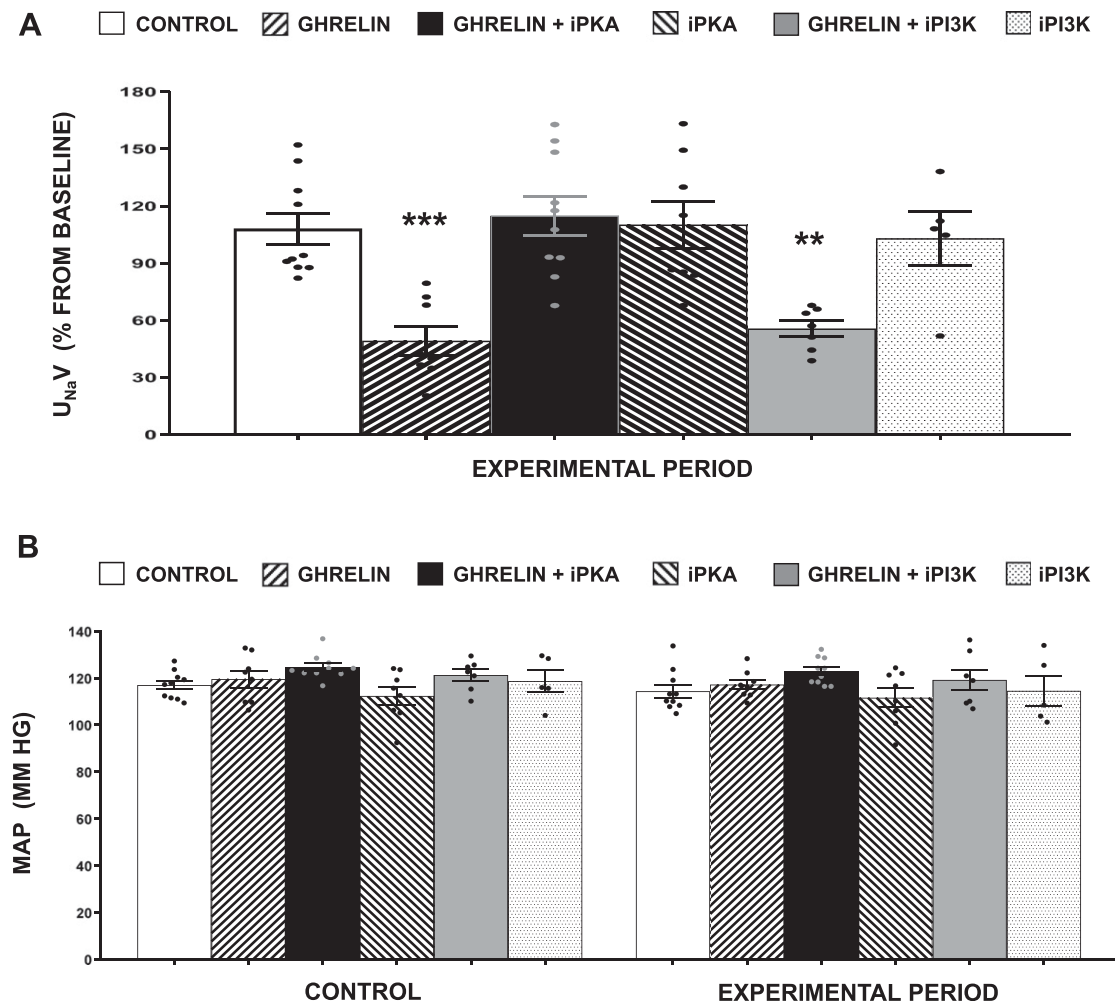


**Figure 1.** (A)  $U_{Na}V$  following the RI infusion of the following (see Keys for bar descriptions): vehicle control D<sub>5</sub>W (n = 10), ghrelin (3  $\mu$ g/min; n = 8), ghrelin + PKA inhibitor (iPKA) Rp-cAMPS (10  $\mu$ g/kg/min; n = 10), iPKA alone (n = 8), ghrelin + PI3K inhibitor (iPI3K) LY (0.1  $\mu$ g/kg/min; n = 7), and iPI3K alone (n = 5). Results are reported as a percentage of own control value. (B) MAP in response to the same infusions as described for A. Results are reported as millimeter of mercury. Data represent means  $\pm$  1 SE. \*\* $P < 0.01$  and \*\*\* $P < 0.001$  from corresponding experimental control period. (A) Overall ANOVA analysis:  $F = 9.3$ ,  $P < 0.0001$ .

any effect on  $U_{Na}V$  when infused alone, and MAP (Fig. 1B) was unaffected by any of the acute RI infusions.

### B. Insulin-Induced pAKT Is Inhibited by LY in IMCD Cells

Insulin is known to stimulate insulin receptors in IMCD cells through the PI3K signaling pathway via pAKT. This set of experiments served to validate the concentration of LY used in our studies to demonstrate effective inhibition of PI3K. As shown in Fig. 2A, insulin treatment significantly increased pAKT levels in two separate experiments [ $0.07 \pm 0.01$  vs  $0.003 \pm 0.0003$  and  $0.06 \pm 0.001$  vs  $0.002 \pm 0.0003$  arbitrary units (AU); both  $P < 0.0001$  from control]. This effect was inhibited in the presence of LY at the concentration used in our *in vivo* ghrelin studies ( $0.07 \pm 0.01$  vs  $0.01 \pm 0.003$  and  $0.06 \pm 0.001$  vs  $0.01 \pm 0.002$  AU; both  $P < 0.0001$ ; representing an inhibition of  $76.5\% \pm 4.1\%$  and  $71.1\% \pm 3.2\%$ , respectively). Compared with control treatment, LY alone demonstrated a nonsignificant decrease in pAKT expression in both experiments. Total AKT expression remained unchanged during all treatments (Fig. 2B), and the increase in the ratio of pAKT/AKT protein expression (each normalized to total protein) in response to insulin ( $P < 0.0001$  vs control for both) was inhibited in the presence of LY treatment (Fig. 2C).

### C. Ghrelin-Induced pSGK<sub>1</sub> Is Abolished in the Presence of PKA Inhibition but Persists During PI3K Inhibition

As shown in Fig. 3A, pSGK<sub>1</sub> a common upstream signaling intermediate regulating  $E_{Na}C$ , significantly increased in response to RI ghrelin infusion compared with vehicle control

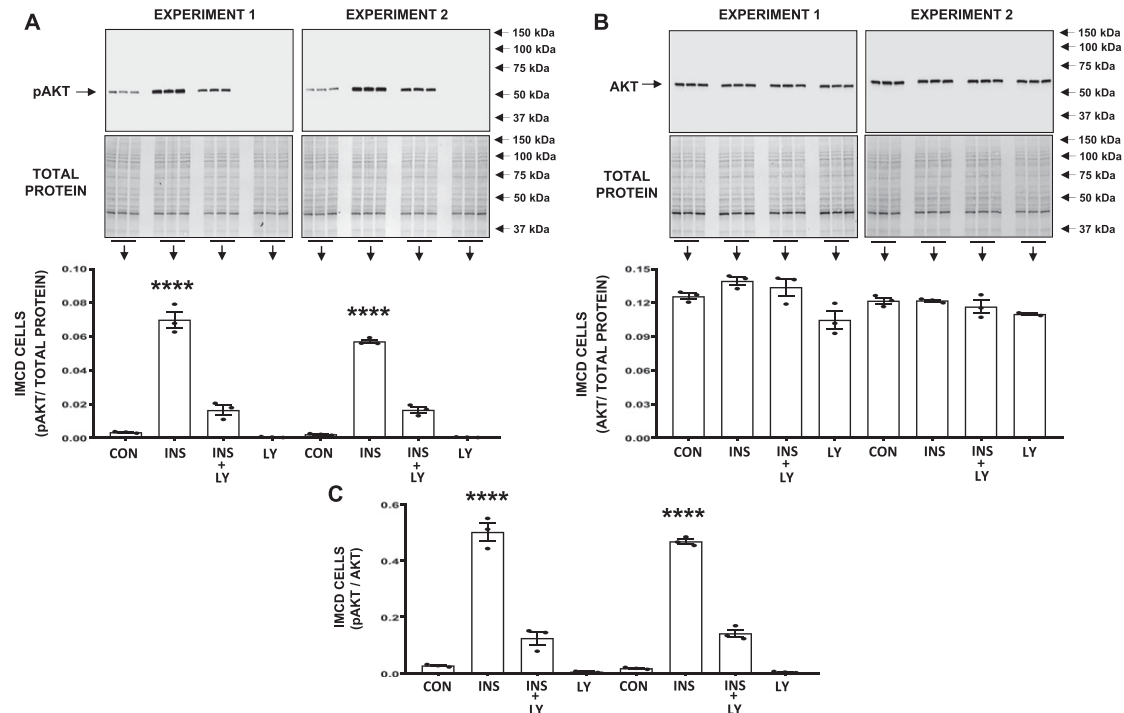


**Figure 2.** (A) Western blot analysis of IMCD cell pAKT following control (CON), insulin (INS; 100 nM), INS + LY (INS [100 nM] + LY [72  $\mu$ M]), and LY from two separate experiments performed in triplicate. (B) Western blot analysis of IMCD cell total AKT for the same four conditions in A. (C) Ratio of pAKT/total AKT (each normalized to total protein) for the same four conditions in A. (A and B) Arrows on the left indicate pAKT and AKT, respectively, whereas arrows on the right depict the molecular weight ladder. Data represent means  $\pm$  1 SE. \*\*\*\* $P < 0.0001$  from control. Overall ANOVA analyses: (A) experiment 1,  $F = 130.8$ ,  $P < 0.0001$ , and experiment 2,  $F = 589.2$ ,  $P < 0.0001$ ; (B) experiment 1,  $F = 138.5$ ,  $P < 0.0001$ , and experiment 2,  $F = 674.8$ ,  $P < 0.0001$ .

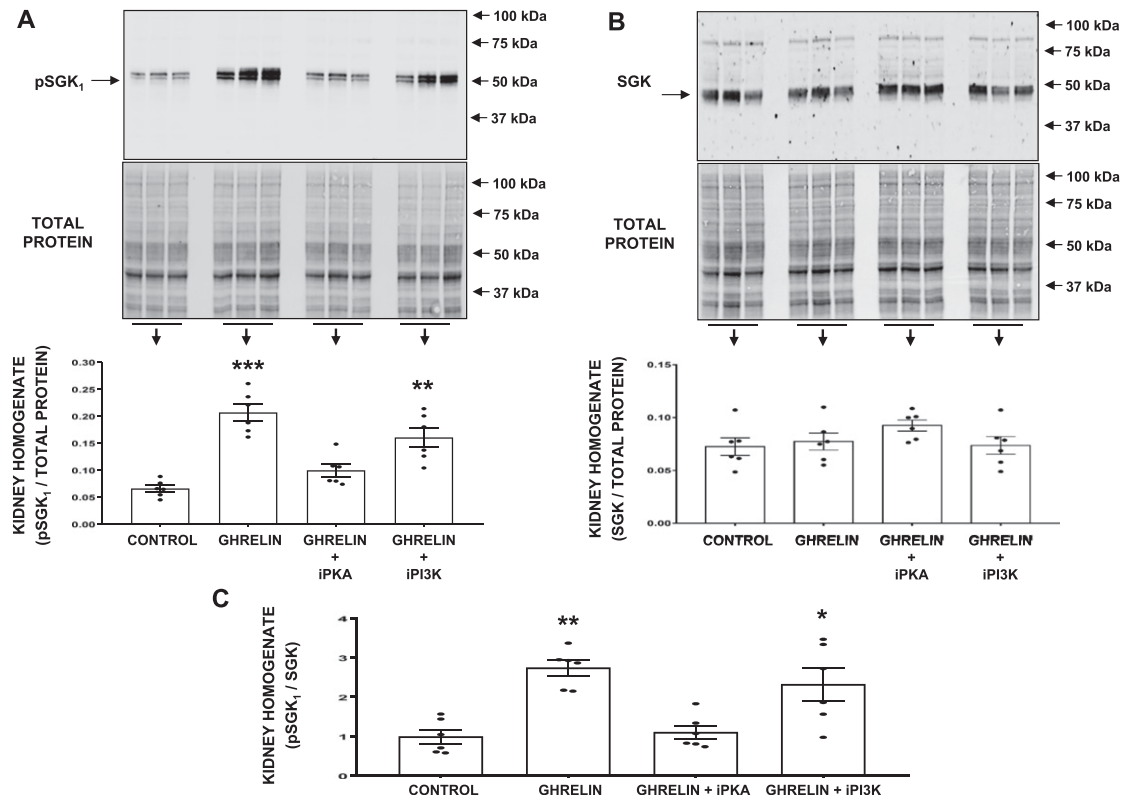


**Figure 3.** (A) Western blot analysis of kidney homogenate pSGK<sub>1</sub> following the RI infusion of the following (n = 6 for each condition): vehicle control D<sub>5</sub>W, ghrelin (3 μg/min), ghrelin + PKA inhibitor (iPKA) Rp-cAMPS (10 μg/kg/min), and ghrelin + PI3K inhibitor (iPI3K) LY (0.1 μg/kg/min). (B) Western blot analysis of kidney homogenate total SGK for the same four conditions in A. (C) Ratio of pSGK<sub>1</sub>/total SGK (each normalized to total protein) for the same four conditions in A. (A and B) Arrows on the left indicate pSGK<sub>1</sub> and SGK, respectively, whereas arrows on the right depict the molecular weight ladder. Data represent means ± 1 SE. \**P* < 0.05, \*\**P* < 0.01, and \*\*\**P* < 0.001 from control. Overall ANOVA analyses: (A) *F* = 21.2, *P* < 0.0001; (B) *F* = 11.4, *P* < 0.0001.

infusion ( $0.21 \pm 0.02$  vs  $0.07 \pm 0.01$  AU; *P* < 0.001). However, during concomitant PKA inhibition, this effect was not observed, and during concomitant PI3K inhibition, the effect remained intact ( $0.16 \pm 0.02$  vs  $0.07 \pm 0.01$  AU; *P* < 0.01). Renal SGK expression remained unaltered following the acute 1-hour RI infusions (Fig. 3B). The increase in the ratio of renal pSGK<sub>1</sub>/SGK protein expression (each normalized to total protein) in response to ghrelin (*P* < 0.01) persisted during PI3K inhibition (*P* < 0.05) but not during ghrelin + PKA inhibition (Fig. 3C).

#### D. Ghrelin-Induced Increases in CD Membrane $\alpha$ E<sub>Na</sub>C Expression Are Abolished in the Presence of PKA Inhibition but Persist During PI3K Inhibition

To determine whether ghrelin induces  $\alpha$ E<sub>Na</sub>C translocation to the plasma membranes of CD cells, we used confocal immunofluorescence microscopy and Western blot analysis. Figure 4A depicts the subcellular distribution of  $\alpha$ E<sub>Na</sub>C, as determined by confocal immunofluorescence microscopy in a representative set of rat CD tubules in response to RI infusions of control, ghrelin, ghrelin + PKA inhibitor, and ghrelin + PI3K inhibitor. Columns (left to right) depict staining for nuclei (blue), AQP-2 (to mark apical membranes of CDs; red),  $\alpha$ E<sub>Na</sub>C (green), and a merged image. RI ghrelin infusion markedly increased  $\alpha$ E<sub>Na</sub>C fluorescence intensity in the apical plasma membrane of CDs compared with control levels (*P* < 0.001; quantified in Fig. 4B). The increase in CD membrane  $\alpha$ E<sub>Na</sub>C fluorescence intensity was abolished during

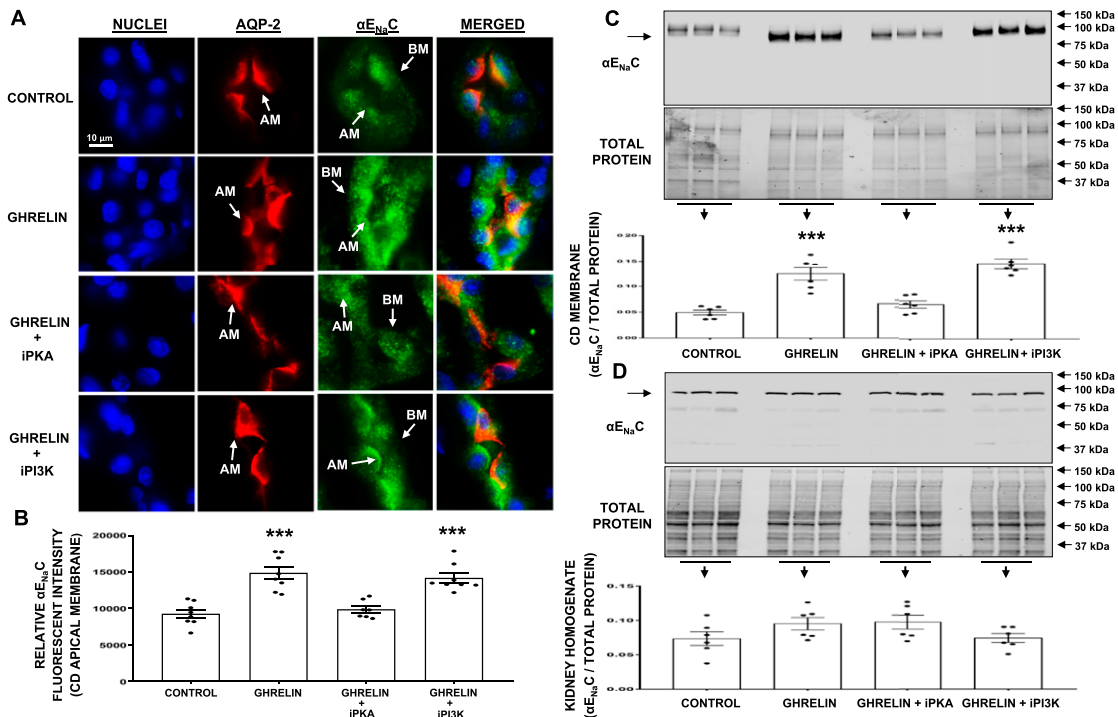


**Figure 4.** (A) Confocal micrographs demonstrating  $\alpha E_{NaC}$  localization in CD cells. Rows of images depict a representative set of CD cells in response to the RI infusion of the following: vehicle control D<sub>5</sub>W, ghrelin (3  $\mu$ g/min), ghrelin + PKA inhibitor (iPKA) Rp-cAMPS (10  $\mu$ g/kg/min), and ghrelin + PI3K inhibitor (iPI3K) LY (0.1  $\mu$ g/kg/min). As indicated, columns (left to right) depict staining for nuclei (blue), AQP-2 (to mark apical membranes of CDs; red),  $\alpha E_{NaC}$  (green), and a merged image. The scale bar in the image represents 10  $\mu$ m. (B) Quantification of CD apical membrane  $\alpha E_{NaC}$  fluorescence intensity. (C and D) Western blot analysis of  $\alpha E_{NaC}$  in CD plasma membranes and kidney homogenate, respectively, in response to the same four conditions in A (n = 6 for each condition). All blots were normalized to total protein. Arrows on the left indicate  $\alpha E_{NaC}$ , whereas arrows on the right depict the molecular weight ladder. Data represent means  $\pm$  1 SE. \*\*\* $P$  < 0.001 from control. Overall ANOVA analyses: (B)  $F = 19.5$ ,  $P < 0.0001$ ; (C)  $F = 27.1$ ,  $P < 0.0001$ . AM, apical membrane; BM, basolateral membrane.

concomitant PKA inhibition ( $P < 0.001$  from ghrelin) but preserved during concomitant PI3K inhibition ( $P < 0.001$  from control), indicating that the increase in membrane  $\alpha E_{NaC}$  in response to ghrelin is dependent on PKA. Furthermore, to complement the immunofluorescence studies on  $\alpha E_{NaC}$  recruitment, we isolated CD plasma membranes using the L<sub>1</sub>CAM pulldown method. Western blot analysis clearly demonstrated  $\alpha E_{NaC}$  recruitment to the CD membranes in response to ghrelin compared with vehicle control ( $0.12 \pm 0.01$  vs  $0.05 \pm 0.01$  AU;  $P < 0.001$ ), which was abolished during concomitant PKA inhibition (Fig. 4C). The ability of ghrelin to increase  $\alpha E_{NaC}$  membrane expression was not affected by concomitant PI3K inhibition ( $0.15 \pm 0.01$  vs  $0.05 \pm 0.01$  AU;  $P < 0.001$ ;  $P =$  not significant from ghrelin). As shown in Fig. 4D, there was no significant difference among vehicle control, ghrelin, ghrelin + PKA inhibitor, or ghrelin + PI3K inhibitor in total renal  $\alpha E_{NaC}$  protein by Western blot analysis, indicating that the increase in CD membrane  $\alpha E_{NaC}$  expression was a result of recruitment and not increased synthesis of  $\alpha E_{NaC}$  in response to ghrelin.

#### *E. Ghrelin-Induced Na<sup>+</sup> Reabsorption Is Abolished in the Presence of Microtubule Polymerization Inhibition but Persists During Actin Polymerization Inhibition*

As shown in Fig. 5, rats received RI infusion of vehicle control D<sub>5</sub>W (n = 10), ghrelin (3  $\mu$ g/minute; n = 8), ghrelin + microtubule inhibitor NOC (3  $\mu$ g/kg/minute; n = 7), ghrelin + actin

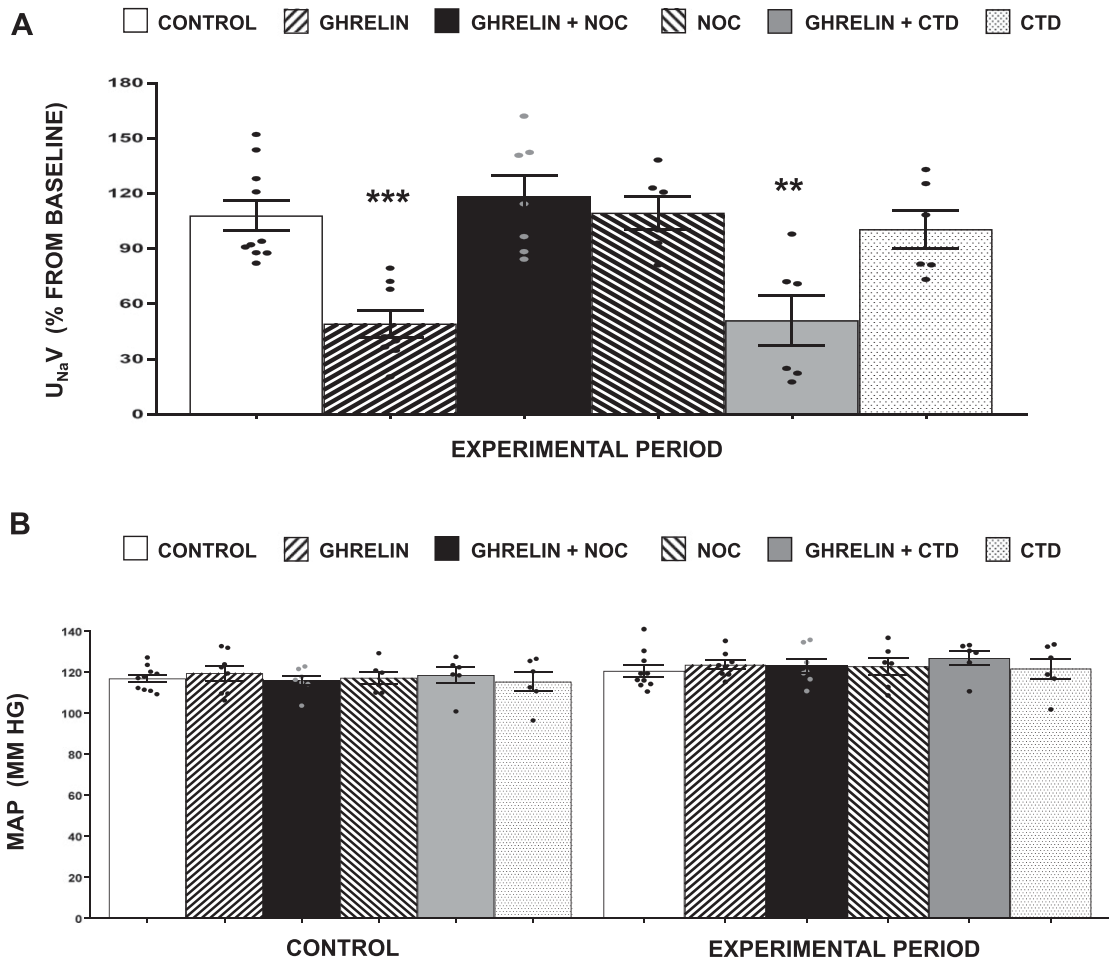


**Figure 5.** (A)  $U_{Na}V$  following the RI infusion of the following (see Keys for bar descriptions): vehicle control D<sub>5</sub>W (n = 10), ghrelin (3  $\mu$ g/min; n = 8), ghrelin + NOC (n = 7), NOC alone (n = 6), ghrelin + CTD (n = 6), and CTD alone (n = 6). Results are reported as a percentage of own control value. (B) MAP in response to the same infusions as described for A. Results are reported as millimeter of mercury. Data represent means  $\pm$  1 SE. \*\* $P$  < 0.01 and \*\*\* $P$  < 0.001 from corresponding experimental control period. (A) Overall ANOVA analysis:  $F = 9.8$ ,  $P < 0.0001$ .

inhibitor CTD (0.3  $\mu$ g/kg/minute; n = 6), NOC alone (n = 6), or CTD alone (n = 6). As shown in Fig. 5A, RI ghrelin infusion induced a significant anti-natriuresis ( $U_{Na}V$  was reduced by  $53.7\% \pm 6.8\%$  compared with vehicle control experimental period;  $P < 0.001$ ); this effect was abolished during concomitant microtubule inhibition with NOC. During ghrelin + actin inhibition with CTD, ghrelin-induced anti-natriuresis persisted ( $U_{Na}V$  was reduced by  $52.8\% \pm 12.7\%$  compared with vehicle control experimental period;  $P < 0.01$ ). Neither NOC nor CTD had any effect on  $U_{Na}V$  when infused alone, and MAP (Fig. 5B) was unaffected by any of the acute RI infusions.

#### *F. Ghrelin-Induced pSGK<sub>1</sub> Persists in the Presence of Both Microtubule and Actin Polymerization Inhibition*

As shown in Fig. 6A, compared with vehicle control-infused kidneys, RI ghrelin significantly increased renal pSGK<sub>1</sub> expression ( $0.11 \pm 0.01$  vs  $0.03 \pm 0.004$  AU;  $P < 0.001$ ). Neither the addition of NOC to inhibit microtubule nor the addition of CTD to inhibit actin polymerization altered the ability of ghrelin to increase pSGK<sub>1</sub> expression ( $0.10 \pm 0.004$  and  $0.09 \pm 0.01$  AU;  $P < 0.001$  and  $P < 0.01$  from vehicle control, respectively). Furthermore, total renal

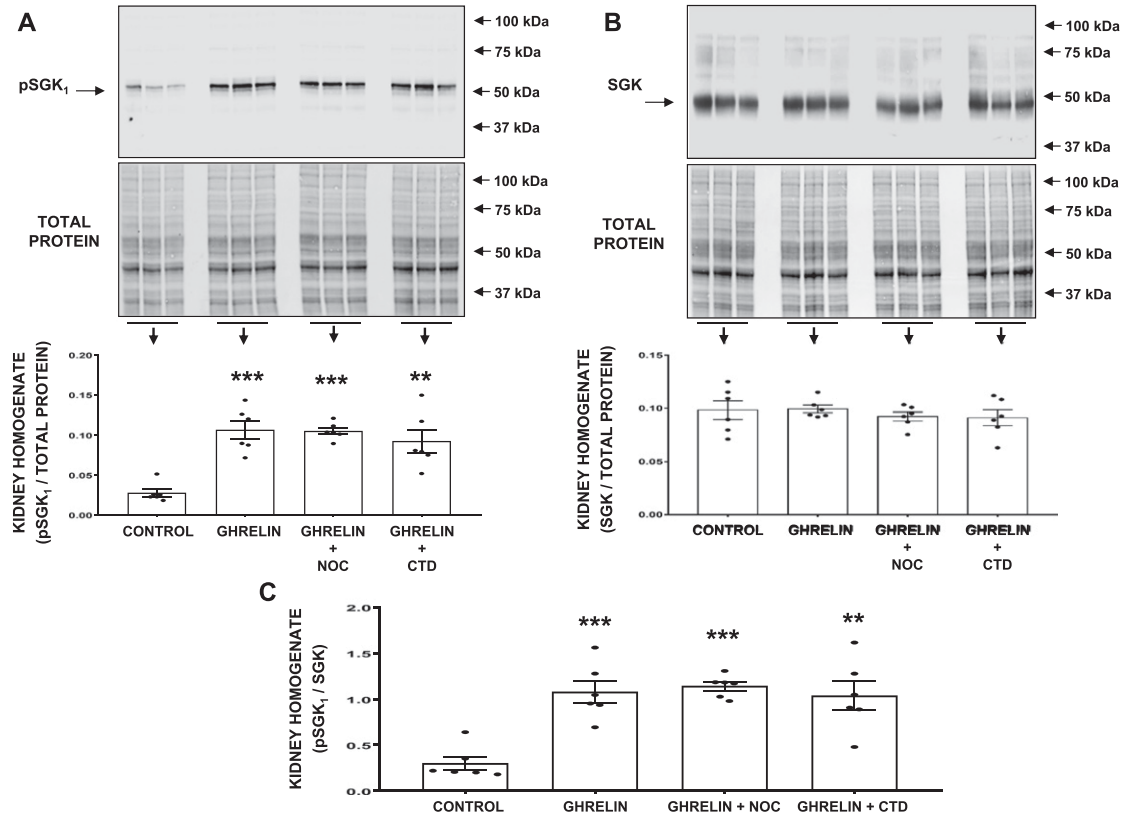


**Figure 6.** (A) Western blot analysis of pSGK<sub>1</sub> in response to the RI infusion of the following (n = 6 for each condition): vehicle control D<sub>5</sub>W, ghrelin (3 μg/min), ghrelin + microtubule inhibitor NOC (3 μg/kg/min), and ghrelin + actin inhibitor CTD (0.3 μg/kg/min). (B) Western blot analysis of total SGK for the same four conditions in A. (C) Ratio of pSGK<sub>1</sub>/total SGK (each normalized to total protein) for the same four conditions in A. (A and B) Arrows on the left indicate pSGK<sub>1</sub> and SGK, respectively, whereas arrows on the right depict the molecular weight ladder. Data represent means ± 1 SE. \*\**P* < 0.01 and \*\*\**P* < 0.001 from control. Overall ANOVA analyses: (A) *F* = 14.9, *P* < 0.0001; (C) *F* = 13.1, *P* < 0.0001.

SGK protein expression remained unchanged in response to any of the infusions (Fig. 6B). Figure 6C depicts the ratio of renal homogenate pSGK<sub>1</sub>/SGK (each normalized to total protein) and demonstrates a significant increase in response to ghrelin, ghrelin + NOC, and ghrelin + CTD infusion (*P* < 0.001, *P* < 0.001, and *P* < 0.01, respectively) when compared with vehicle control infusion.

#### G. RI Infusion of NOC and CTD Inhibit Microtubule and Actin Polymerization

To verify inhibition of microtubule polymerization by NOC and actin polymerization by CTD, confocal microscopy was performed to measure α-tubulin and β-actin immunofluorescence. As indicated in Fig. 7A, columns (left to right) depict staining for AQP-2 (to mark apical membranes of CDs; green), α-tubulin (red), a merged image, an enlarged merged image (×3) of the square box in the preceding merged image, and an enlarged image for α-tubulin staining alone, each following RI infusions of control, ghrelin, and ghrelin + NOC. RI ghrelin + NOC infusion demonstrated a significant reduction in the α-tubulin immunofluorescent signal in CD cells after 1 hour (32.3% ± 5.5% reduction; *P* < 0.01 from control and ghrelin, quantified in Fig. 7B), thereby confirming disruption of microtubule polymerization. Ghrelin alone had no effect on microtubule polymerization. As indicated in Fig. 7C, columns (left to right) depict staining for AQP-2 (to mark apical membranes of CDs; green), β-actin (red), a merged image, an enlarged merged image (×3) of the square box in the preceding

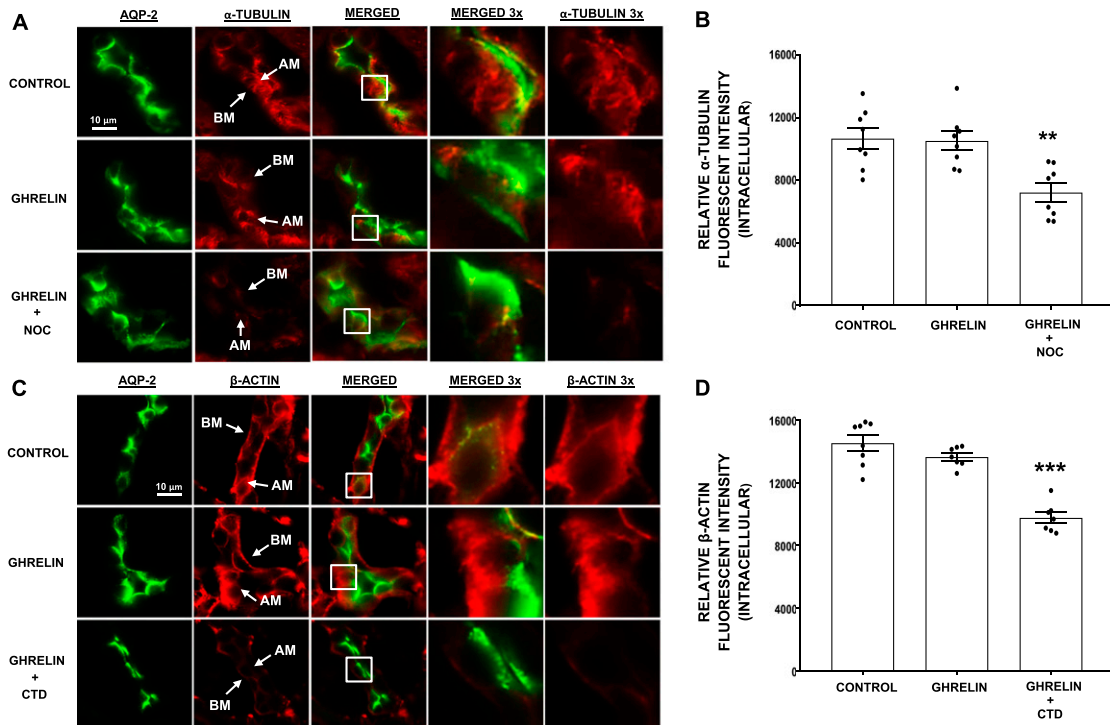


**Figure 7.** (A) Confocal micrographs demonstrating  $\alpha$ -tubulin localization in CD cells. Rows of images depict a representative set of CD cells in response to the RI infusion of the following: vehicle control D<sub>5</sub>W, ghrelin (3  $\mu$ g/min), and ghrelin + microtubule inhibitor NOC (3  $\mu$ g/kg/min). As indicated, columns (left to right) depict staining for AQP-2 (to mark apical membrane CDs; green),  $\alpha$ -tubulin (red), a merged image, an enlarged merged image ( $\times 3$ ) of the square section that appears in the original merged image, and an enlarged image with  $\alpha$ -tubulin alone. The scale bar in the image represents 10  $\mu$ m. (B) Quantification of CD  $\alpha$ -tubulin fluorescence intensity. (C) Confocal micrographs demonstrating  $\beta$ -actin localization in CD cells. Rows of images depict a representative set of CD cells in response to the RI infusion of the following: vehicle control D<sub>5</sub>W, ghrelin (3  $\mu$ g/min), and ghrelin + actin inhibitor CTD (0.3  $\mu$ g/kg/min). As indicated, columns (left to right) depict staining for AQP-2 (to mark apical membranes of CDs; green),  $\beta$ -actin (red), a merged image, an enlarged merged image ( $\times 3$ ) of the square section that appears in the original merged image, and an enlarged image with  $\beta$ -actin alone. The scale bar in the image represents 10  $\mu$ m. (D) Quantification of CD  $\beta$ -actin fluorescence intensity. Data represent means  $\pm$  1 SE. \*\* $P < 0.01$  and \*\*\* $P < 0.001$  from control. Overall ANOVA analyses: (B)  $F = 9.8$ ,  $P < 0.0001$ ; (D)  $F = 41.4$ ,  $P < 0.0001$ . AM, apical membrane; BM, basolateral membrane.

merged image, and an enlarged merged image for  $\beta$ -actin staining alone, each following the RI infusions of control, ghrelin, and ghrelin + CTD. RI ghrelin + CTD infusion demonstrated a significant reduction in the  $\beta$ -actin signal in CD cells after 1 hour ( $32.8\% \pm 2.5\%$  reduction;  $P < 0.001$  from control and ghrelin, quantified in Fig. 7D), thereby confirming disruption of actin polymerization. Ghrelin alone had no effect on actin polymerization.

#### H. Ghrelin-Induced Increases in CD Membrane $\alpha$ E<sub>Na</sub>C Expression Are Abolished During Inhibition of Microtubule Polymerization but Not Actin Polymerization

To determine whether ghrelin induces  $\alpha$ E<sub>Na</sub>C translocation to the plasma membrane of CD cells, we used confocal immunofluorescence microscopy and Western blot analysis. Figure 8A, depicts the subcellular distribution of  $\alpha$ E<sub>Na</sub>C as determined by confocal immunofluorescence microscopy in a representative set of rat CD tubules in response to the RI infusions of vehicle, ghrelin, ghrelin + microtubule inhibitor NOC, and ghrelin + actin inhibitor CTD. As indicated, columns (left to right) depict staining for nuclei (blue), AQP-2 (to mark apical membranes of CDs; red),  $\alpha$ E<sub>Na</sub>C (green), and a merged image. RI ghrelin infusion markedly

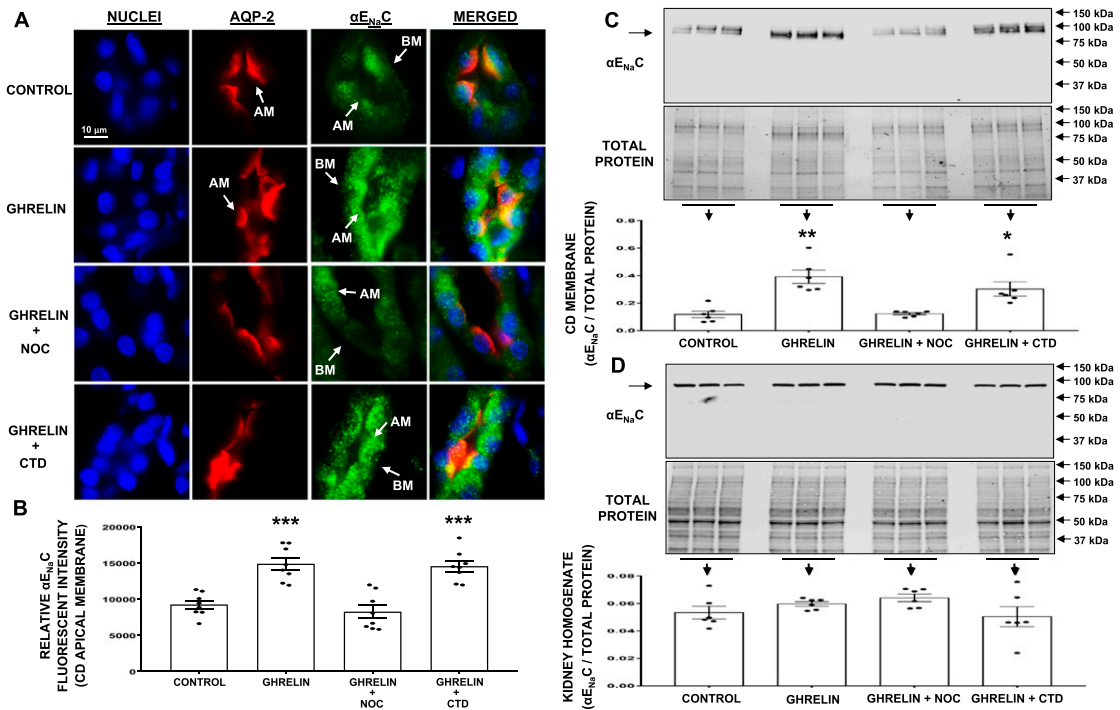


**Figure 8.** (A) Confocal micrographs demonstrating  $\alpha E_{Na}C$  localization in CD cells. Rows of images depict a representative set of CD cells in response to the RI infusion of the following: vehicle control D<sub>5</sub>W, ghrelin (3  $\mu$ g/min), ghrelin + microtubule inhibitor NOC (3  $\mu$ g/kg/min), and ghrelin + actin inhibitor CTD (0.3  $\mu$ g/kg/min). As indicated, columns (left to right) depict staining for nuclei (blue), AQP-2 (to mark apical membranes of CDs; red),  $\alpha E_{Na}C$  (green), and a merged image. The scale bar in the image represents 10  $\mu$ m. (B) Quantification of CD apical membrane  $\alpha E_{Na}C$  fluorescence intensity. (C and D) Western blot analysis of  $\alpha E_{Na}C$  in CD plasma membranes and kidney homogenate, respectively, in response to the same four conditions in A (n = 6 for each condition). All blots were normalized to total protein. Arrows on the left indicate  $\alpha E_{Na}C$ , whereas arrows on the right depict the molecular weight ladder. Data represent means  $\pm$  1 SE. \* $P$  < 0.05, \*\* $P$  < 0.01, and \*\*\* $P$  < 0.001 from control. Overall ANOVA analyses: (B)  $F$  = 20.1,  $P$  < 0.0001; (C)  $F$  = 13.1,  $P$  < 0.0001. AM, apical membrane; BM, basolateral membrane.

increased  $\alpha E_{Na}C$  fluorescence intensity in the apical plasma membrane of CDs compared with control levels ( $P$  < 0.001; quantified in Fig. 8B). The increase in CD apical membrane  $\alpha E_{Na}C$  fluorescence intensity was abolished during concomitant microtubule inhibition with NOC ( $P$  < 0.01 from ghrelin) but preserved during concomitant actin inhibition with CTD ( $P$  < 0.001 from control), indicating that the increase in apical membrane  $\alpha E_{Na}C$  in response to ghrelin is microtubule dependent. Furthermore, to complement the immunofluorescence studies on  $\alpha E_{Na}C$  recruitment, we isolated CD membranes using the L<sub>1</sub>CAM pull-down method (Fig. 8C). Western blot analysis also demonstrated  $\alpha E_{Na}C$  recruitment to the CD membranes in response to ghrelin compared with control (0.39  $\pm$  0.05 vs 0.12  $\pm$  0.02 AU;  $P$  < 0.01), an effect that was abolished during microtubule polymerization inhibition. The ability of ghrelin to increase  $\alpha E_{Na}C$  expression was not affected by actin polymerization inhibition (0.30  $\pm$  0.05 vs 0.12  $\pm$  0.02 AU;  $P$  < 0.05). As shown in Fig. 8D, total renal  $\alpha E_{Na}C$  expression remained unchanged in response to any of the infusions, indicating that the increase in CD membrane  $\alpha E_{Na}C$  expression was a result of recruitment and not increased synthesis of  $\alpha E_{Na}C$  in response to ghrelin.

#### *I. Neither Total nor pNedd4-2 Is Altered by RI Ghrelin or Ghrelin + Cytoskeletal Disruption With NOC or CTD*

pNedd4-2 decreases  $E_{Na}C$  channel removal from the plasma membranes of CD cells via interference with the  $E_{Na}C$ -Nedd4-2 interaction. In response to RI ghrelin infusion, neither

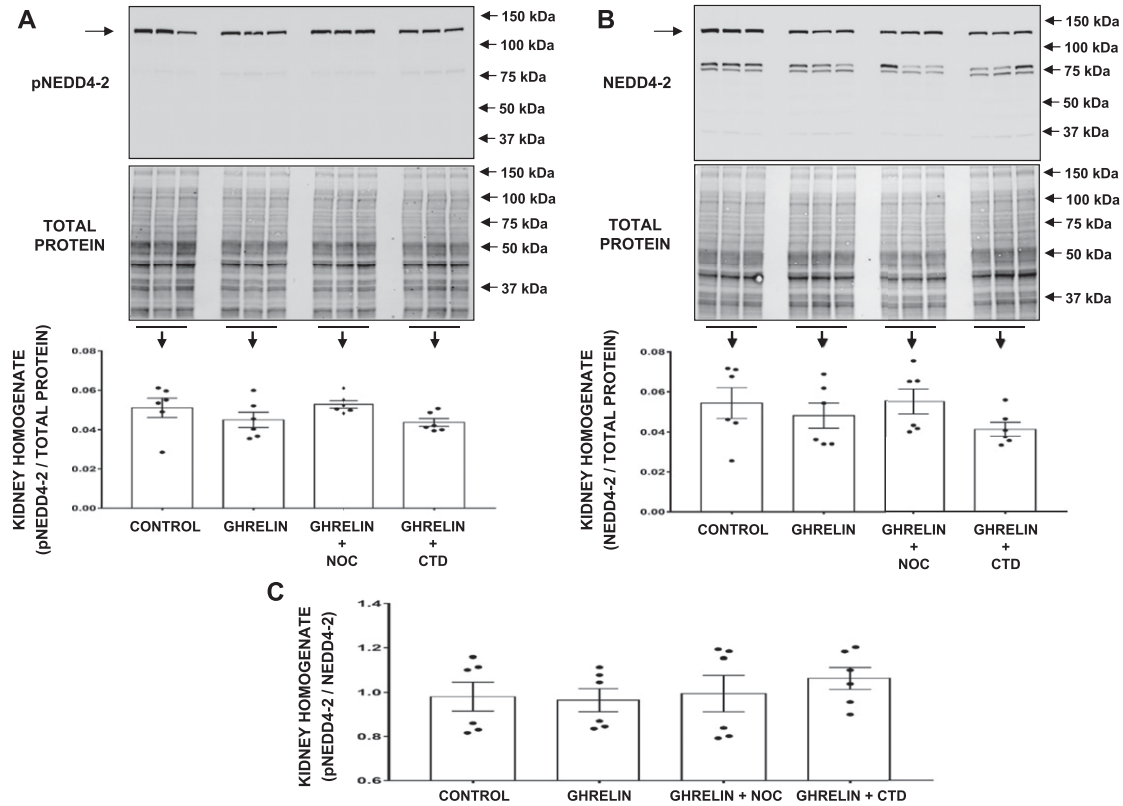


**Figure 9.** (A) Western blot analysis of kidney homogenate pNedd4-2 in response to the RI infusion of the following ( $n = 6$  for each condition): vehicle control  $D_5W$ , ghrelin ( $3 \mu\text{g}/\text{min}$ ), ghrelin + microtubule inhibitor NOC ( $3 \mu\text{g}/\text{kg}/\text{min}$ ), and ghrelin + actin inhibitor CTD ( $0.3 \mu\text{g}/\text{kg}/\text{min}$ ). (B) Western blot analysis of kidney homogenate total Nedd4-2 for the same four conditions in A. (C) Ratio of pNedd4-2/total Nedd4-2 (each normalized to total protein) for the same four conditions in A. (A and B) Arrows on the left indicate pNedd4-2 and total Nedd4-2, respectively, whereas arrows on the right depict the molecular weight ladder. Data represent means  $\pm 1$  SE.

pNedd4-2 nor total Nedd4-2 protein expression was changed. Furthermore, neither the addition of NOC nor the addition of CTD to ghrelin failed to alter pNedd4-2 or total renal Nedd4-2 in these studies (Fig. 9A–9C).

### 3. Discussion

The key findings of the present studies are as follows: (i) ghrelin-induced anti-natriuresis, pSGK<sub>1</sub>, and increases in membrane expression of  $\alpha E_{\text{Na}}\text{C}$  are mediated by PKA and not PI3K in the rat kidney; (ii) the lack of change in total renal  $\alpha E_{\text{Na}}\text{C}$  expression and pNedd4-2 suggests that ghrelin-induced anti-natriuresis is a result of  $\alpha E_{\text{Na}}\text{C}$  translocation to the CD plasma membrane; and (iii) whereas the pSGK<sub>1</sub>, in response to ghrelin, is resistant to cytoskeletal disruption, both the anti-natriuresis and  $\alpha E_{\text{Na}}\text{C}$  translocation are dependent on an intact microtubule (rather than actin) network. Taken together, these studies elucidate the pathway that connects cAMP to  $\alpha E_{\text{Na}}\text{C}$  in GR-mediated  $\text{Na}^+$  reabsorption within the kidney and serve to identify ghrelin as a hormonal regulator of microtubule-dependent forward trafficking of  $\alpha E_{\text{Na}}\text{C}$  (Fig. 10).

Extrarenal GRs are known to activate two distinct signaling cascades: adenylyl cyclase/cAMP [36] and phospholipase C/protein kinase C [37]. cAMP-dependent GR effects have been reported in the hypothalamus [38], where GRs increase food intake, and in the pancreas, where they regulate insulin secretion in islets [39]. In pituitary somatotrophs, however, GRs

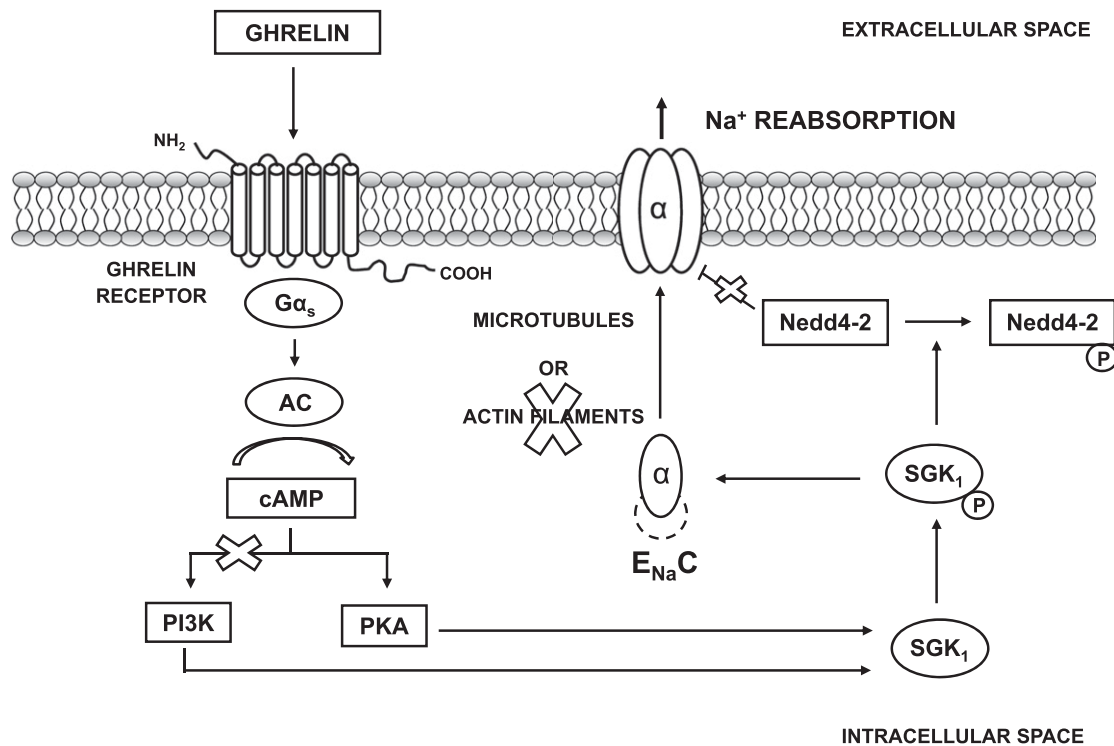


**Figure 10.** Summary schematic depicting the proposed mechanisms of ghrelin-induced anti-natriuresis. AC, adenylyl cyclase; encircled P, phosphorylated.

signal through a phospholipase C-dependent pathway [38], thus supporting the concept of tissue-specific GR signaling. In the kidney, previous studies have demonstrated that GR-induced  $\text{Na}^+$  reabsorption is mediated by adenylyl cyclase (with increases in microdialysate cAMP levels) but not by protein kinase C [1]. cAMP can mediate pSGK<sub>1</sub> by both PKA and PI3K in the CD, but the present studies have identified PKA as the mediator of ghrelin-induced pSGK<sub>1</sub>.

PKA in CD cells is known to mediate a host of responses, the most established of which is water reabsorption that occurs from vasopressin binding to its V2 receptor, promoting forward trafficking of AQP-2 [40]. This effect is dependent on the “release” of vesicular AQP-2 and resultant plasma membrane insertion of AQP-2 [41]. Whereas the direct effect of vasopressin to phosphorylate SGK<sub>1</sub> has not been reported, the possibility of PKA representing a convergence point between CD  $\text{Na}^+$  reabsorption via ghrelin-induced  $E_{\text{NaC}}$  translocation and CD water reabsorption via vasopressin-induced AQP-2 translocation is certainly intriguing. Furthermore, as potassium excretion via Ang II effects at the Ang II Type 1 receptor [42] and urea transporter effects to regulate urine concentrating ability [43] in the CD are also mediated by the cAMP–PKA pathway, identification of PKA in the signaling pathway of ghrelin in the CD adds yet another layer of complexity to our current understanding of the regulation of urinary composition.

The pSGK<sub>1</sub>, in response to ghrelin, has been shown in previous studies [1, 4], but its mediation by PKA and lack of sensitivity to microtubule or actin disruption have not. Unlike most serine-threonine kinases, SGK<sub>1</sub> is under dual control: total protein levels are controlled through effects on its gene transcription, whereas its activity is dependent on phosphorylation, either via PI3K or PKA. In the acute setting, the main effect of aldosterone is to increase  $E_{\text{NaC}}$  activity via its upregulation of total SGK<sub>1</sub> protein levels in ion-transporting epithelia [44]; insulin and other activators of the PI3K, however, are key regulators of its activity via phosphorylation of previously synthesized SGK<sub>1</sub> [45]. *In vivo*, SGK<sub>1</sub> has been shown to be phosphorylated in response to insulin via the PI3K pathway [46], but a hormonal

stimulus for PKA-mediated pSGK<sub>1</sub> *in vivo* has not. Furthermore, cytoskeletal disruption did not affect pSGK<sub>1</sub> in response to ghrelin, suggesting that these components are not necessary for pSGK<sub>1</sub> in our studies. Microtubule disruption did, however, inhibit ghrelin-induced anti-natriuresis and increases in CD membrane  $\alpha\text{E}_{\text{Na}}\text{C}$  expression, indicating that this machinery is more important to the portion of the ghrelin pathway distal to pSGK<sub>1</sub>.

Following intrarenal ghrelin infusion, CD plasma membrane  $\alpha\text{E}_{\text{Na}}\text{C}$  expression was significantly increased, but total renal  $\alpha\text{E}_{\text{Na}}\text{C}$  expression remained unchanged. This has been shown in other studies during high-fat diet-induced hypertension [2] and Ang II-induced hypertension [4] as well. In the current acute studies, we used two complementary methods to confirm increased membrane  $\alpha\text{E}_{\text{Na}}\text{C}$  expression in response to RI ghrelin infusion. First, capitalizing on the specificity of the L<sub>1</sub>CAM epitope for the outer plasma membranes of CD principal cells (and not distal tubule cells) [26], we pulled down outer CD membranes and subsequently probed for  $\alpha\text{E}_{\text{Na}}\text{C}$  protein expression in this fraction. We compared this with total renal  $\alpha\text{E}_{\text{Na}}\text{C}$  expression, which remained unchanged. We also demonstrated increased plasma membrane  $\alpha\text{E}_{\text{Na}}\text{C}$  expression in response to ghrelin using confocal microscopy imaging techniques. Both methodologies revealed increased plasma membrane  $\alpha\text{E}_{\text{Na}}\text{C}$  expression in response to ghrelin.

Accumulating evidence suggests that  $\text{E}_{\text{Na}}\text{C}$  trafficking is controlled by a series of kinase-mediated signaling pathways that regulate the distribution of the channel between intracellular compartments and the apical membrane [47]. These kinases respond to multiple systemic and local signals, and there is a critical need to identify the stimuli that control  $\text{E}_{\text{Na}}\text{C}$  trafficking. This goal has only been achieved to any substantial degree in the case of the endocytic mediator, Nedd4-2, yet there are multiple steps in the forward trafficking pathways subsequent to  $\text{E}_{\text{Na}}\text{C}$  endocytosis that impact membrane  $\text{E}_{\text{Na}}\text{C}$  density. These processes are relatively untapped compared with our knowledge of Nedd4-2 regulation. As pSGK<sub>1</sub> can regulate  $\alpha\text{E}_{\text{Na}}\text{C}$  activity by affecting the abundance of the protein in the plasma membrane of CD cells, we examined factors that would promote stability at the CD cell surface [14], as well as induce trafficking to the CD cell surface. In the first most studied situation, pSGK<sub>1</sub> binds to the ubiquitin-protein ligase Nedd4-2 and phosphorylates it, interfering with the  $\alpha\text{E}_{\text{Na}}\text{C}$ -Nedd4-2 interaction [15]. The subsequent reduction in  $\alpha\text{E}_{\text{Na}}\text{C}$  ubiquitinylation and internalization leads to accumulation of  $\alpha\text{E}_{\text{Na}}\text{C}$  channels at the apical plasma membrane. In our studies, we found no difference in the pNedd4-2 in response to ghrelin but were able to demonstrate a reduction in ghrelin-induced membrane  $\alpha\text{E}_{\text{Na}}\text{C}$  expression during microtubule inhibition with NOC. As pSGK<sub>1</sub> can directly induce the insertion of  $\alpha\text{E}_{\text{Na}}\text{C}$  into the plasma membrane via a microtubule-dependent mechanism [48], it is likely that ghrelin is one of the hormones regulating this response.

In conclusion, the present studies have elucidated the signaling pathway underlying ghrelin-induced  $\text{Na}^+$  reabsorption in the kidney. The increase in translocation of  $\alpha\text{E}_{\text{Na}}\text{C}$  in response to ghrelin is crucial to our understanding of disorders characterized by increased  $\text{E}_{\text{Na}}\text{C}$ -mediated  $\text{Na}^+$  reabsorption, such as hyperaldosteronism, Liddle's syndrome, pregnancy-induced hypertension, obesity nephropathy, and congestive heart failure. Furthermore, having established the signaling pathways linking ghrelin to  $\text{Na}^+$  reabsorption, we now have a foundation upon which to investigate  $\text{Na}^+$ -independent actions of ghrelin in the kidney. These include, but are not limited to, ghrelin-mediated regulation of inflammatory markers and sympathetic nervous system output (as have been reported for ghrelin in extrarenal tissues).

## Acknowledgments

**Financial Support:** Support for this work was provided by the National Institutes of Health Grant R01DK110369 (to S.H.P.).

## Additional Information

**Correspondence:** Shetal H. Padia, MD, Division of Endocrinology and Metabolism, Department of Medicine, P.O. Box 801414, University of Virginia Health System, Charlottesville, Virginia 22908. E-mail: [shp6a@virginia.edu](mailto:shp6a@virginia.edu).

**Disclosure Summary:** The authors have nothing to disclose.

**Data Availability:** All data generated or analyzed during this study are included in this published article or in the data repositories listed in References.

---

## References and Notes

- Kemp BA, Howell NL, Gildea JJ, Keller SR, Padia SH. Intrarenal ghrelin receptors regulate ENaC-dependent sodium reabsorption by a cAMP-dependent pathway. *Kidney Int.* 2013;**84**(3):501–508.
- Kemp BA, Howell NL, Gildea JJ, Padia SH. Intrarenal ghrelin receptor antagonism prevents high-fat diet-induced hypertension in male rats. *Endocrinology.* 2014;**155**(7):2658–2666.
- Kemp BA, Howell NL, Gray JT, Keller SR, Nass RM, Padia SH. Intrarenal ghrelin infusion stimulates distal nephron-dependent sodium reabsorption in normal rats. *Hypertension.* 2011;**57**(3):633–639.
- Kemp BA, Howell NL, Padia SH. Intrarenal ghrelin receptor inhibition ameliorates angiotensin II-dependent hypertension in rats. *Am J Physiol Renal Physiol.* 2018;**315**(4):F1058–F1066.
- Faletti CJ, Perrotti N, Taylor SI, Blazer-Yost BL. sgk: an essential convergence point for peptide and steroid hormone regulation of ENaC-mediated Na<sup>+</sup> transport. *Am J Physiol Cell Physiol.* 2002;**282**(3):C494–C500.
- Helms MN, Fejes-Toth G, Naray-Fejes-Toth A. Hormone-regulated transepithelial Na<sup>+</sup> transport in mammalian CCD cells requires SGK1 expression. *Am J Physiol Renal Physiol.* 2003;**284**(3):F480–F487.
- Kobayashi T, Cohen P. Activation of serum- and glucocorticoid-regulated protein kinase by agonists that activate phosphatidylinositide 3-kinase is mediated by 3-phosphoinositide-dependent protein kinase-1 (PDK1) and PDK2. *Biochem J.* 1999;**339**(2):319–328.
- Park J, Leong ML, Buse P, Maiyar AC, Firestone GL, Hemmings BA. Serum and glucocorticoid-inducible kinase (SGK) is a target of the PI 3-kinase-stimulated signaling pathway. *EMBO J.* 1999;**18**(11):3024–3033.
- Perrotti N, He RA, Phillips SA, Haft CR, Taylor SI. Activation of serum- and glucocorticoid-induced protein kinase (Sgk) by cyclic AMP and insulin. *J Biol Chem.* 2001;**276**(12):9406–9412.
- Vasquez MM, Castro R, Seidner SR, Henson BM, Ashton DJ, Mustafa SB. Induction of serum- and glucocorticoid-induced kinase-1 (SGK1) by cAMP regulates increases in alpha-ENaC. *J Cell Physiol.* 2008;**217**(3):632–642.
- Gonzalez-Robayna IJ, Falender AE, Ochsner S, Firestone GL, Richards JS. Follicle-stimulating hormone (FSH) stimulates phosphorylation and activation of protein kinase B (PKB/Akt) and serum and glucocorticoid-induced kinase (Sgk): evidence for A kinase-independent signaling by FSH in granulosa cells. *Mol Endocrinol.* 2000;**14**(8):1283–1300.
- Canessa CM, Merillat AM, Rossier BC. Membrane topology of the epithelial sodium channel in intact cells. *Am J Physiol.* 1994;**267**(6):C1682–C1690.
- Schild L, Canessa CM, Shimkets RA, Gautschi I, Lifton RP, Rossier BC. A mutation in the epithelial sodium channel causing Liddle disease increases channel activity in the *Xenopus laevis* oocyte expression system. *Proc Natl Acad Sci USA.* 1995;**92**(12):5699–5703.
- Tiwari S, Nordquist L, Halagappa VK, Ecelbarger CA. Trafficking of ENaC subunits in response to acute insulin in mouse kidney. *Am J Physiol Renal Physiol.* 2007;**293**(1):F178–F185.
- Snyder PM, Olson DR, Kabra R, Zhou R, Steines JC. cAMP and serum and glucocorticoid-inducible kinase (SGK) regulate the epithelial Na<sup>(+)</sup> channel through convergent phosphorylation of Nedd4-2. *J Biol Chem.* 2004;**279**(44):45753–45758.
- Pochynyuk O, Staruschenko A, Bugaj V, Lagrange L, Stockand JD. Quantifying RhoA facilitated trafficking of the epithelial Na<sup>+</sup> channel toward the plasma membrane with total internal reflection fluorescence-fluorescence recovery after photobleaching. *J Biol Chem.* 2007;**282**(19):14576–14585.
- Sasaki S, Yui N, Noda Y. Actin directly interacts with different membrane channel proteins and influences channel activities: AQP2 as a model. *Biochim Biophys Acta.* 2014;**1838**(2):514–520.
- RRID:AB\_10917439, [http://scicrunch.org/resolver/AB\\_10917439](http://scicrunch.org/resolver/AB_10917439).
- RRID:AB\_477521, [http://scicrunch.org/resolver/AB\\_477521](http://scicrunch.org/resolver/AB_477521).
- RRID:AB\_2149325, [http://scicrunch.org/resolver/AB\\_2149325](http://scicrunch.org/resolver/AB_2149325).
- RRID:AB\_10698593, [http://scicrunch.org/resolver/AB\\_10698593](http://scicrunch.org/resolver/AB_10698593).
- RRID:AB\_2801582, [http://scicrunch.org/resolver/AB\\_2801582](http://scicrunch.org/resolver/AB_2801582).
- RRID:AB\_772210, [http://scicrunch.org/resolver/AB\\_772210](http://scicrunch.org/resolver/AB_772210).
- RRID:AB\_772206, [http://scicrunch.org/resolver/AB\\_772206](http://scicrunch.org/resolver/AB_772206).
- RRID:AB\_448025, [http://scicrunch.org/resolver/AB\\_448025](http://scicrunch.org/resolver/AB_448025).
- Helbert MJ, Dauwe SE, De Broe ME. Flow cytometric immunodissection of the human distal tubule and cortical collecting duct system. *Kidney Int.* 2001;**59**(2):554–564.

27. RRID:AB\_2536183, [http://scicrunch.org/resolver/AB\\_2536183](http://scicrunch.org/resolver/AB_2536183).
28. RRID:AB\_141607, [http://scicrunch.org/resolver/AB\\_141607](http://scicrunch.org/resolver/AB_141607).
29. RRID:AB\_301662, [http://scicrunch.org/resolver/AB\\_301662](http://scicrunch.org/resolver/AB_301662).
30. RRID:AB\_477583, [http://scicrunch.org/resolver/AB\\_477583](http://scicrunch.org/resolver/AB_477583).
31. RRID:AB\_2285600, [http://scicrunch.org/resolver/AB\\_2285600](http://scicrunch.org/resolver/AB_2285600).
32. RRID:AB\_2810957, [http://scicrunch.org/resolver/AB\\_2810957](http://scicrunch.org/resolver/AB_2810957).
33. RRID:AB\_2223172, [http://scicrunch.org/resolver/AB\\_2223172](http://scicrunch.org/resolver/AB_2223172).
34. RRID:AB\_2315049, [http://scicrunch.org/resolver/AB\\_2315049](http://scicrunch.org/resolver/AB_2315049).
35. RRID:AB\_329827, [http://scicrunch.org/resolver/AB\\_329827](http://scicrunch.org/resolver/AB_329827).
36. Howard AD, Feighner SD, Cully DF, Arena JP, Liberators PA, Rosenblum CI, Hamelin M, Hreniuk DL, Palyha OC, Anderson J, Paress PS, Diaz C, Chou M, Liu KK, McKee KK, Pong SS, Chaung LY, Elbrecht A, Dashkevich M, Heavens R, Rigby M, Sirinathsinghji DJ, Dean DC, Melillo DG, Patchett AA, Nargund R, Griffin PR, DeMartino JA, Gupta SK, Schaeffer JM, Smith RG, Van der Ploeg LH. A receptor in pituitary and hypothalamus that functions in growth hormone release. *Science*. 1996; **273**(5277):974–977.
37. Adams EF, Petersen B, Lei T, Buchfelder M, Fahlbusch R. The growth hormone secretagogue, L-692,429, induces phosphatidylinositol hydrolysis and hormone secretion by human pituitary tumors. *Biochem Biophys Res Commun*. 1995; **208**(2):555–561.
38. Kohno D, Gao HZ, Muroya S, Kikuyama S, Yada T. Ghrelin directly interacts with neuropeptide-Y-containing neurons in the rat arcuate nucleus: Ca<sup>2+</sup> signaling via protein kinase A and N-type channel-dependent mechanisms and cross-talk with leptin and orexin. *Diabetes*. 2003; **52**(4):948–956.
39. Dezaki K, Damdindorj B, Sone H, Dyachok O, Tengholm A, Gylfe E, Kurashina T, Yoshida M, Kakei M, Yada T. Ghrelin attenuates cAMP-PKA signaling to evoke insulinostatic cascade in islet  $\beta$ -cells. *Diabetes*. 2011; **60**(9):2315–2324.
40. Vukićević T, Schulz M, Faust D, Klusmann E. The trafficking of the water channel aquaporin-2 in renal principal cells—a potential target for pharmacological intervention in cardiovascular diseases. *Front Pharmacol*. 2016; **7**:23.
41. Geraghty KM, Chen S, Harthill JE, Ibrahim AF, Toth R, Morrice NA, Vandermoere F, Moorhead GB, Hardie DG, MacKintosh C. Regulation of multisite phosphorylation and 14-3-3 binding of AS160 in response to IGF-1, EGF, PMA and AICAR. *Biochem J*. 2007; **407**(2):231–241.
42. Wei Y, Liao Y, Zavilowitz B, Ren J, Liu W, Chan P, Rohatgi R, Estilo G, Jackson EK, Wang WH, Satlin LM. Angiotensin II type 2 receptor regulates ROMK-like K<sup>+</sup> channel activity in the renal cortical collecting duct during high dietary K<sup>+</sup> adaptation. *Am J Physiol Renal Physiol*. 2014; **307**(7):F833–F843.
43. Su H, Chen M, Sands JM, Chen G. Activation of the cAMP/PKA pathway induces UT-A1 urea transporter monoubiquitination and targets it for lysosomal degradation. *Am J Physiol Renal Physiol*. 2013; **305**(12):F1775–F1782.
44. Quinn S, Harvey BJ, Thomas W. Rapid aldosterone actions on epithelial sodium channel trafficking and cell proliferation. *Steroids*. 2014; **81**:43–48.
45. Pearce D. SGK1 regulation of epithelial sodium transport. *Cell Physiol Biochem*. 2003; **13**(1):13–20.
46. Huang J, Ledford KJ, Pitkin WB, Russo L, Najjar SM, Siragy HM. Targeted deletion of murine CEACAM 1 activates PI3K-Akt signaling and contributes to the expression of (pro)renin receptor via CREB family and NF- $\kappa$ B transcription factors. *Hypertension*. 2013; **62**(2):317–323.
47. Butterworth MB, Edinger RS, Frizzell RA, Johnson JP. Regulation of the epithelial sodium channel by membrane trafficking. *Am J Physiol Renal Physiol*. 2009; **296**(1):F10–F24.
48. Diakov A, Korbmacher C. A novel pathway of epithelial sodium channel activation involves a serum- and glucocorticoid-inducible kinase consensus motif in the C terminus of the channel's alpha-subunit. *J Biol Chem*. 2004; **279**(37):38134–38142.